

# Equation of state and hybrid star properties with the weakly interacting light U-boson in relativistic models

Dong-Rui Zhang<sup>1</sup>, Wei-Zhou Jiang<sup>1</sup>, Si-Na Wei<sup>1</sup>, Rong-Yao Yang<sup>1</sup>, Qian-Fei Xiang<sup>2</sup>

<sup>1</sup> *Department of Physics, Southeast University, Nanjing 211189, China*

<sup>2</sup> *Institute of High Energy Physics, Chinese Academy of Sciences, Beijing 100049, China*

It has been a puzzle whether quarks may exist in the interior of massive neutron stars, since the hadron-quark phase transition softens the equation of state (EOS) and reduce the neutron star (NS) maximum mass very significantly. In this work, we consider the light U-boson that increases the NS maximum mass appreciably through its weak coupling to fermions. The inclusion of the U-boson may thus allow the existence of the quark degrees of freedom in the interior of large mass neutron stars. Unlike the consequence of the U-boson in hadronic matter, the stiffening role of the U-boson in the hybrid EOS is not sensitive to the choice of the hadron phase models. In addition, we have also investigated the effect of the effective QCD correction on the hybrid EOS. This correction may reduce the coupling strength of the U-boson that is needed to satisfy NS maximum mass constraint. While the inclusion of the U-boson also increases the NS radius significantly, we find that appropriate in-medium effects of the U-boson may reduce the NS radii significantly, satisfying both the NS radius and mass constraints well.

PACS numbers: 26.60.Kp, 21.60.Jz, 97.60.Jd

## I. INTRODUCTION

The equation of state (EOS) of isospin asymmetric nuclear matter is of prime importance for the investigation of nuclear structure [1–4], heavy-ion reaction dynamics [5, 6], and many issues in astrophysics [6–11]. However, the EOS of asymmetric matter at supra-normal densities are still poorly known [6, 12], though the constraint on the symmetric part of the EOS at supra-normal densities can be extracted from the collective flow data of high energy heavy-ion reactions [13]. Different models and approaches can produce rather different high-density behaviors [14–17], while the complexity arises for the EOS of asymmetric matter when the phase transitions, such as hyperon productions, meson condensations, and quark deconfinement, take place at high densities. Normally, phase transitions can soften the EOS and reduce the neutron star (NS) maximum mass significantly.

Recently, massive NS's, for instance, the pulsars PSR J1614-2230 with  $M = 1.97 \pm 0.04 M_{\odot}$  [18], and PSR J0348+0432, with  $M = 2.01 \pm 0.04 M_{\odot}$  [19] were identified with the high-precision measurements. The larger NS mass means the stiffer EOS of NS matter at high densities. Considering the phase transitions in the NS core and the EOS constraint from the collective flow data at high densities, it is difficult for the nuclear models to reproduce NS's as massive as  $2M_{\odot}$ . This indeed proposes a challenge to the nuclear EOS at supra-normal densities. One may doubt whether there are new degrees of freedom besides nucleons in NS's [18, 20, 21]. On the other hand, one may contemplate

what interactions can allow the new degrees of freedom in massive NS's [22–35].

The mixture of low-density hadronic matter and high-density quark matter may form in the NS core after the hadron-quark transition occurs with the increase of density. In order to evade the potential conflict between the softened EOS due to the appearance of the quark phase and the observed massive NS's, it is necessary to stiffen the quark EOS, for instance, by considering the strong coupling and/or color superconductivity [24–29, 32]. Recently, a new repulsion, provided by the U-boson, was introduced for nucleons in NS's [36–38]. The light U-boson, first proposed by Fayet [39], might be regarded as the mediator of the putative fifth force [40–42]. Recently, this light U-boson has been considered as the interaction mediator of the MeV dark matter to account for the bright 511 keV  $\gamma$ -ray from the galactic bulge [43–46]. The coupling of the U-boson with the nucleons is very weak, but can increase appreciably the NS maximum mass [36–38] and influence the transition density at the inner edge separating the liquid core from the solid crust, effectively [47]. In particular, the weak coupling to baryons plays a striking role in stabilizing neutron stars in the presence of the super-soft symmetry energy [37] that is extracted from the FOPI/GSI data on the  $\pi^-/\pi^+$  ratio in relativistic heavy-ion collisions [48].

In this work, we consider the effect of the U-boson on the softened EOS due to the hadron-quark phase transition. We adopt the relativistic mean-field (RMF) theory, which achieved great success in the past few decades [49–58], to describe hadronic matter, and the MIT bag model for quark matter [59, 60]. For the hadron-quark phase transition, we use Gibbs construction [61, 62] to determine the mixed phase of hadronic and quark matter. As the stiffening role of the U-boson depends on the softness of the models [38], we will examine how the U-boson stiffens the hybrid EOS's initiated with different hadronic models. Since quarks in the bag model are free of interaction, it is also interesting to investigate briefly the effect of the effective correction from the perturbative QCD [26, 63–66]. Eventually, we will investigate the properties of hybrid stars with various EOS's and discuss how the mass and radius constraints of the NS observations can be satisfied. The paper is organized as follows. In Sec. II, we present briefly the formalism. In Sec. III, numerical results and discussions are presented. At last, a summary is given in Sec. IV.

## II. FORMALISM

In the RMF models we adopted in this work, the nucleon-nucleon interaction is realized via the exchange of three mesons: the isoscalar meson  $\sigma$ , which provides the intermediate-range attraction between the nucleons, the isoscalar-vector meson  $\omega$ , which offers the short-range repulsion, and the isovector-vector meson  $b_0$ , which accounts for the isospin dependence of the nuclear force. Though the  $\pi$  meson interacts strongly with nucleons, we do not include it here because the RMF framework

just has the Hartree term that gives a zero contribution of the pseudoscalar meson. The  $\pi$  mesons can be included in the relativistic Hartree-Fock approximation. Without the exchange terms, the RMF approximation still works well due mainly to the fact that in the relativistic framework the fermions are already identified by the Dirac equation that is specifically for fermions. Moreover, the interaction in the RMF approximation, built upon the equilibrium between the intermediate-range attraction and the short-range repulsion, can yield the saturation properties of nuclear matter very well [49–55]. The relativistic Lagrangian is then written as:

$$\begin{aligned}\mathcal{L} = & \bar{\psi}[i\gamma_\mu\partial^\mu - M + g_\sigma\sigma - g_\omega\gamma_\mu\omega^\mu - g_\rho\gamma_\mu\tau_3b_0^\mu]\psi \\ & - \frac{1}{4}F_{\mu\nu}F^{\mu\nu} + \frac{1}{2}m_\omega^2\omega_\mu\omega^\mu - \frac{1}{4}B_{\mu\nu}B^{\mu\nu} + \frac{1}{2}m_\rho^2b_{0\mu}b_0^\mu \\ & + \frac{1}{2}(\partial_\mu\sigma\partial^\mu\sigma - m_\sigma^2\sigma^2) + U_{\text{eff}}(\sigma, \omega^\mu, b_0^\mu) + \mathcal{L}_u,\end{aligned}\quad (1)$$

where  $\psi, \sigma, \omega, b_0$  are the fields of the nucleon, scalar, vector, and neutral isovector-vector mesons, with their masses  $M, m_\sigma, m_\omega$ , and  $m_\rho$ , respectively.  $g_i (i = \sigma, \omega, \rho)$  are the corresponding meson-nucleon couplings.  $F_{\mu\nu}$  and  $B_{\mu\nu}$  are the strength tensors of  $\omega$  and  $\rho$  mesons respectively,

$$F_{\mu\nu} = \partial_\mu\omega_\nu - \partial_\nu\omega_\mu, \quad B_{\mu\nu} = \partial_\mu b_{0\nu} - \partial_\nu b_{0\mu}. \quad (2)$$

The self-interacting terms of  $\sigma, \omega$  mesons and the isoscalar-isovector coupling are given generally as

$$\begin{aligned}U_{\text{eff}}(\sigma, \omega^\mu, b_0^\mu) = & -\frac{1}{3}g_2\sigma^3 - \frac{1}{4}g_3\sigma^4 + \frac{1}{4}c_3(\omega_\mu\omega^\mu)^2 \\ & + 4\Lambda_V g_\rho^2 g_\omega^2 \omega_\mu\omega^\mu b_{0\mu}b_0^\mu.\end{aligned}\quad (3)$$

In addition, we include in the Lagrangian  $\mathcal{L}_u$  for the U-boson that is beyond the standard model. Following the form of the vector meson,  $\mathcal{L}_u$  is written as:

$$\mathcal{L}_u = -\bar{\psi}g_u\gamma_\mu u^\mu\psi - \frac{1}{4}U_{\mu\nu}U^{\mu\nu} + \frac{1}{2}m_u^2 u_\mu u^\mu, \quad (4)$$

with  $u$  the field of U-boson.  $U_{\mu\nu}$  is the strength tensor of U-boson,

$$U_{\mu\nu} = \partial_\mu u_\nu - \partial_\nu u_\mu. \quad (5)$$

With the standard Euler-Lagrange formalism, we can deduce from the Lagrangian the equations of motion for the nucleon and meson fields. While in the mean-field approximation the Dirac field of nucleons is quantized [52], the fields of mesons and U-boson, which are replaced by their classical expectation values, obey following equations:

$$m_\sigma^2\sigma = g_\sigma\rho_s - g_2\sigma^2 - g_3\sigma^3, \quad (6)$$

$$m_\omega^2\omega_0 = g_\omega\rho_B - c_3\omega_0^3 - 8\Lambda_V g_\rho^2 g_\omega^2 b_0^2\omega_0, \quad (7)$$

$$m_\rho^2b_0 = g_\rho\rho_3 - 8\Lambda_V g_\rho^2 g_\omega^2 \omega_0^2 b_0, \quad (8)$$

$$m_u^2u_0 = g_u\rho_B, \quad (9)$$

where the temporal subscript of the  $\rho$  meson is neglected for convenience,  $\rho_s$  and  $\rho_B$  are the scalar and baryon densities, respectively, and  $\rho_3$  is the difference between the proton and neutron densities, namely,  $\rho_3 = \rho_p - \rho_n$ . The set of coupled equations can be solved self-consistently using the iteration method. With these mean-field quantities, the resulting energy density  $\varepsilon$  and pressure  $P$  for the hadronic phase are written as:

$$\begin{aligned} \varepsilon = & \sum_{i=p,n} \frac{2}{(2\pi)^3} \int^{k_{F_i}} d^3k E_i^* + \frac{1}{2} m_\omega^2 \omega_0^2 + \frac{1}{2} \frac{g_u^2}{m_u^2} \rho_B^2 + \frac{1}{2} m_\sigma^2 \sigma^2 + \frac{1}{2} m_\rho^2 b_0^2 \\ & + \frac{1}{3} g_2 \sigma^3 + \frac{1}{4} g_3 \sigma^4 + \frac{3}{4} c_3 \omega_0^4 + 12 \Lambda_V g_\rho^2 g_\omega^2 \omega_0^2 b_0^2, \end{aligned} \quad (10)$$

$$\begin{aligned} P = & \frac{1}{3} \sum_{i=p,n} \frac{2}{(2\pi)^3} \int^{k_{F_i}} d^3k \frac{\mathbf{k}^2}{E_i^*} + \frac{1}{2} m_\omega^2 \omega_0^2 + \frac{1}{2} \frac{g_u^2}{m_u^2} \rho_B^2 - \frac{1}{2} m_\sigma^2 \sigma^2 + \frac{1}{2} m_\rho^2 b_0^2 \\ & - \frac{1}{3} g_2 \sigma^3 - \frac{1}{4} g_3 \sigma^4 + \frac{1}{4} c_3 \omega_0^4 + 4 \Lambda_V g_\rho^2 g_\omega^2 \omega_0^2 b_0^2, \end{aligned} \quad (11)$$

with  $E_i^* = \sqrt{\mathbf{k}^2 + (M_i^*)^2}$ .

For the quark phase, we use the MIT bag model, in which the unique parameter, the bag constant, arises from the energy difference between the perturbative ground state and the chiral symmetry breaking vacuum of the theory [67]. In addition to its simplicity, the MIT bag model has been widely used because of its success in describing the vacuum properties of hadrons. As the hadron-quark phase transition occurs, the hadronic degrees of freedom starts to turn into quarks which are free of interactions in the bag model. The pressure and energy density are given as:

$$\begin{aligned} \varepsilon_Q = & B + \sum_f \frac{3}{4\pi^2} [\mu_f (\mu_f^2 - m_f^2)^{1/2} (\mu_f^2 - \frac{1}{2} m_f^2) - \frac{1}{2} m_f^4 \ln(\frac{\mu_f + (\mu_f^2 - m_f^2)^{1/2}}{m_f})] \\ & + \frac{1}{2} \frac{g_u^2}{m_u^2} \rho_Q^2, \end{aligned} \quad (12)$$

$$\begin{aligned} P_Q = & -B + \sum_f \frac{1}{4\pi^2} [\mu_f (\mu_f^2 - m_f^2)^{1/2} (\mu_f^2 - \frac{5}{2} m_f^2) + \frac{3}{2} m_f^4 \ln(\frac{\mu_f + (\mu_f^2 - m_f^2)^{1/2}}{m_f})] \\ & + \frac{1}{2} \frac{g_u^2}{m_u^2} \rho_Q^2. \end{aligned} \quad (13)$$

where  $B$  is the bag constant,  $\rho_Q$  is the density of quarks, and the sum runs over the flavor  $f$ . With the perturbative QCD correction included to the first order [26, 63–66], the grand thermodynamic potentials for quarks are given as

$$\Omega_u = -\frac{\mu_u^4}{4\pi^2} (1 - c), \quad (14)$$

$$\Omega_d = -\frac{\mu_d^4}{4\pi^2} (1 - c), \quad (15)$$

$$\Omega = \sum_{f=u,d,s} \Omega_f + B, \quad (16)$$

where the term linear in  $c = 2\alpha_s/\pi$  is from the perturbative QCD correction, and the masses of up and down quarks are set to zero in obtaining above expressions. Due to the nonzero strange quark

mass ( $m_s = 150 \text{ MeV}$  in the calculation of this work), the expression for the  $\Omega_s$  is a little tedious and can be referred to Ref. [63]. All thermodynamic quantities follow consistently from the  $\Omega$ . Since quark matter in hybrid stars is not in the perturbative regime, we regard  $c$  and the bag constant as effective parameters in the present model, and denote the effective perturbative QCD correction simply as the QCD correction in the following. The pressure is given by  $P(\mu) = -\Omega(\mu)$ , the quark number density by  $n(\mu) = \partial P / \partial \mu$ , and the energy density by  $\varepsilon = -P + \mu n$ .

We use Gibbs construction [61, 62] to depict the hadron-quark phase transition. After the hadron-quark phase transition sets in, one may construct a mixed phase of hadronic and quark matter over a finite range of pressures and densities according to the Gibbs conditions for phase equilibrium. The Gibbs conditions for the chemical and mechanical equilibriums and the charge neutral condition are written as

$$\mu_b b_i - \mu_c q_i = \mu_i, \quad (17)$$

$$P_H = P_Q, \quad (18)$$

$$(1 - Y) \sum_b \rho_b q_b + \frac{Y}{3} \sum_f \rho_f q_f + \sum_l \rho_l q_l = 0, \quad (19)$$

where  $i$  runs over baryons, leptons ( $b_i = 0$  for leptons) and quarks, and  $Y$  is the baryon number fraction of the quark phase. With these conditions, the onset density of the hadron-quark phase transition can be obtained, and the mixed phase is then constructed. Eventually, the total baryon density, energy density and pressure of the mixed phase are in turn given by

$$(1 - Y) \sum_b \rho_b + \frac{Y}{3} \sum_f \rho_f = \rho, \quad (20)$$

$$\varepsilon_M = (1 - Y)\varepsilon_H + Y\varepsilon_Q + \varepsilon_l, \quad (21)$$

$$P_M = (1 - Y)P_H + YP_Q + P_l. \quad (22)$$

Note that one may also use the Maxwell construction for the phase transition. However, the Maxwell construction does not have the mixed phase. In the Maxwell construction, a direct transition from hadronic to quark matter is accompanied by a density jump and both phases are separately charge neutral. Regardless of the charge chemical equilibrium, only a single (baryon) chemical potential is common to the hadronic and quark phases with a constant pressure. To avoid the motion of charge due to the different charge chemical potentials in two phases in the Maxwell construction, a more realistic equation of state can be obtained from the Wigner-Seitz cell calculation by taking into account the Coulomb and surface effects. Then, the equation of state of the mixed phase obtained from this approach becomes close to that of the Gibbs construction [34].

Using the EOS of hybrid star matter as an input, we may obtain the NS properties by solving the

Tolman-Oppenheimer-Volkoff (TOV) equation [68, 69]:

$$\frac{dP(r)}{dr} = -\frac{[P(r) + \varepsilon(r)][M(r) + 4\pi r^3 P(r)]}{r(r - 2M(r))}, \quad (23)$$

$$M(r) = 4\pi \int_0^r \tilde{r}^2 \varepsilon(\tilde{r}) d\tilde{r}, \quad (24)$$

where  $r$  is the radial coordinate from the center of the star,  $P(r)$  and  $\varepsilon(r)$  are the pressure and energy density at the position  $r$ , respectively, and  $M(r)$  is the mass contained in the sphere of the radius  $r$ . Note that here we use units for which the gravitation constant is  $G_\infty = c = 1$ . The radius  $R$  and mass  $M(R)$  of a NS are obtained from the condition  $p(R) = 0$ . Because the NS matter undergoes a phase transition from the homogeneous matter to the inhomogeneous matter at the low density region, the EOS obtained from the homogeneous matter does not apply to the low density region and the empirical low-density EOS in the literature [70, 71] is adopted.

### III. RESULTS AND DISCUSSIONS

For the hadronic phase in hybrid stars, we consider the simple compositions: neutrons, protons, electrons and muons. We do not include hyperons in this work. The appearance of hyperons can largely soften the equation of state, thus reducing the mass of neutron stars greatly. Due to the accurate mass measurement of large-mass neutron stars, people even conclude that the hyperon EOS has to be ruled out [18]. Indeed, the onset densities of hyperons are very model-dependent. With the RMF parameter set NL3, the  $\Lambda$  hyperon appears at about  $0.28 fm^{-3}$  [72, 73], while it is at about  $0.48 fm^{-3}$  with the extended MDI interaction [74]. The superfluidity of hyperons renders the  $\Lambda$  hyperons to appear at around  $0.64 fm^{-3}$  [75], which just affects the properties of neutron star slightly. When the hyperonic degrees of freedom are included, it is found that the hadron-quark transition density can not change continuously with the emergence of hyperons. This means that the appearance of hyperons disfavors the hadron-quark phase transition in the RMF models. Similar effect of the hyperons is found in the literature [76]. As implied by the large-mass NS's, the in-medium hyperon potential should be density-dependent [23]. We may further explore the density-dependent interaction of hyperons in the future and it is beyond the scope of the present work.

Among a number of nonlinear RMF models, we select two typical best-fit parameter sets, NL3 [77] and FSUGold [78], to describe the hadron phase of hybrid star matter. Parameters and saturation properties of these two parameter sets are listed in Table I. Usually, the nonlinear RMF models include the nonlinear self-interacting meson terms to simulate appropriate in-medium effect of the strong interaction. The parameter set NL3 includes the nonlinear self-interaction of the  $\sigma$  meson, while in addition to the latter, the nonlinear self-interaction of the  $\omega$  meson is also included in FSUGold. The resulting EOS of the FSUGold is much softer than that of the NL3 at high densities.

It is known before that the vector U-boson can stiffen the EOS, and the stiffening role is much more significant for the soft EOS in pure hadronic matter [38]. It is thus interesting to see whether we can observe a similar phenomenon in hybrid star matter, if hadronic phase is described with these two different RMF models.

TABLE I: Parameters and saturation properties for the hadron phase models NL3 and FSUGold. Meson masses, incompressibility  $\kappa$  and symmetry energy are in units of MeV, and the density is in unit of  $fm^{-3}$ .

	$g_\sigma$	$g_\omega$	$g_\rho$	$m_\sigma$	$m_\omega$	$m_\rho$	$g_2$	$g_3$	$c_3$	$\Lambda_V$	$\rho_0$	$\kappa$	$M^*/M$	$E_{sym}$
NL3	10.217	12.868	4.474	508.194	782.501	763	10.431	-28.890	-	-	0.148	271.8	0.60	37.4
FSUGold	10.592	14.302	5.884	491.500	782.500	763	4.277	49.934	418.39	0.03	0.148	230.0	0.61	32.5

While it is still an open question to determine the density at which the hadron-quark phase transition occurs, we investigate the onset of the phase transition in two manners: one is to fix the transition density  $\rho_c$  by adjusting the bag constant, and the other to fix the bag constant. Given the bag constant, we also obtain the transition density which is now dependent on the hadron phase models. Once the transition density is determined, we can construct the mixed phase with the Gibbs conditions and then obtain the EOS of hybrid star matter.

In this work, we choose the bag constant to be  $B^{1/4} = 180 \sim 220$  MeV which is a reasonable range between those values by fitting the light-hadron spectra [79–82] and those (e.g., 250 MeV) used in the hydrodynamical evolution of the quark gluon plasma [83, 84]. The present range is also close to that used in the literature [32, 74, 85]. For the choice of the transition density, we are referred to the literature where it is around  $1.5 \sim 4\rho_0$  [26, 86–88]. In addition to the fact that the EOS of hybrid star matter with a transition density  $4\rho_0$  or even higher just has a minor effect on the star maximum mass, we choose the range ( $2 \sim 3\rho_0$ ) for the transition density in this work.

As an example, we calculate here the various phase boundaries with  $B^{1/4} = 180$  MeV and with the transition densities  $2\rho_0$  and  $3\rho_0$ . For the parameter set NL3, the transition density with  $B^{1/4} = 180$  MeV from the hadronic phase to the mixed phase is about  $0.20 fm^{-3}$ , and  $0.77 fm^{-3}$  from the mixed phase to pure quark phase. The extent of the mixed phase is about  $0.57 fm^{-3}$ . For the parameter set FSUGold, the extent of the mixed phase is  $1.47 fm^{-3}$  with the onset transition density  $0.28 fm^{-3}$ . For the case with the transition density fixed at  $2\rho_0$ , the extent of the mixed phase is about  $0.95 fm^{-3}$  with the parameter set NL3, while it is  $1.7 fm^{-3}$  with the parameter set FSUGold. For the transition density at  $3\rho_0$ , the extents of the mixed phase are  $1.99 fm^{-3}$  and  $2.34 fm^{-3}$  with the NL3 and FSUGold, respectively.

The phase transition usually tends to soften the EOS, as is consistent with the requirement of spontaneous stability in natural processes. This is also true for the hadron-quark phase transition in isospin asymmetric nuclear matter. In Fig. 1, we depict the EOS of hybrid star matter for various

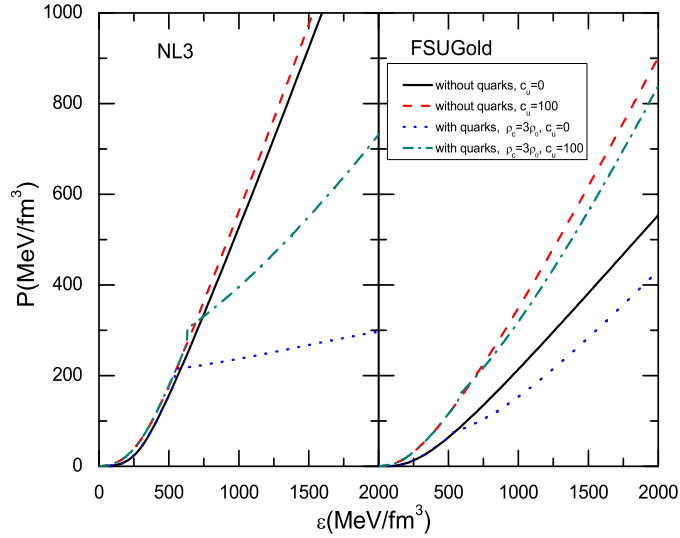


FIG. 1: (Color online) Equation of state of NS matter with and without quarks. The curves with the U-boson contribution are also shown for comparisons. The value of the ratio parameter  $c_u = (g_u/m_u)^2$  is in unit of  $\text{GeV}^{-2}$ . The hadronic matter EOS is obtained with the NL3 (left panel) and FSUGold (right panel).

cases with the onset density  $3\rho_0$  for hadron-quark phase transition. In comparison to the EOS without phase transition as shown in Fig. 1, we see that the EOS of isospin asymmetric matter is greatly softened by the hadron-quark phase transition. It is striking to see that the stiff EOS with the NL3, which is not favored by the constraint from the flow data of the heavy-ion reactions [13], even becomes much softer than the soft FSUGold EOS due to the hadron-quark transition. With the inclusion of the U-boson, the soft EOS is stiffened greatly. Because the EOS of hybrid star matter initiated with the NL3 is now much softer than that with the FSUGold, the stiffening effect turns out to be much more appreciable for the EOS initiated with the NL3. The similar stiffening role of the U-boson can also be clearly seen in the case without phase transition, as we compare curves with the NL3 and FSUGold. Since the softening of the EOS due to the hadron-quark phase transition reduces largely the maximum mass of NS's, we will see below that the inclusion of the U-boson plays an important role in satisfying the maximum mass constraint for NS's.

To see the role of the U-boson specifically, we depict in Fig. 2 the EOS's of hybrid star matter for a set of the ratio parameter  $c_u = (g_u/m_u)^2$ . Similar to that shown in Fig. 1, the EOS of hybrid star matter is stiffened significantly due to the repulsion provided by the U-boson. We see that the EOS with the soft (FSUGold) and stiff (NL3) hadron phase models acquires similar stiffening especially for the case with the fixed bag constant. This is different from the case in pure hadronic matter where a much more significant stiffening effect is produced by the soft model [38]. While for the case with the fixed transition density, the stiffening role of U-boson is more significant for the stiff parameter set NL3. The reason for these to occur lies in the following facts. In pure hadronic matter with RMF models, there is the cancelation between the repulsion provided by the vector meson and



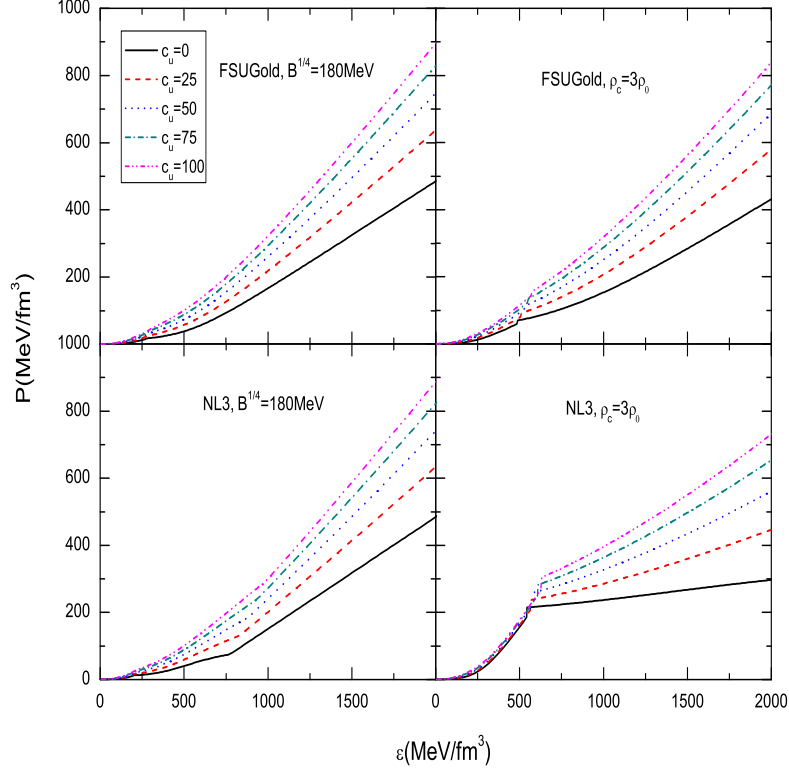


FIG. 2: (Color online) Equation of state of hybrid star matter. The hadronic phase is given by two RMF parameter sets, NL3 (lower panels) and FSUGold (upper panels). For quark phase, we present the results with the fixed bag constant (left panels) and fixed transition density (right panels). In each panel, the various curves are obtained with different ratio parameters  $c_u$ .

the attraction provided by the scalar meson. Thus, more significant cancelation in the soft model sharpens the importance of the repulsion provided by the U-boson. While quarks are modeled by the MIT bag model with the same bag constant, the repulsion provided by the U-boson plays the same stiffening role in the quark phase EOS, after the hadron-quark phase transition occurs. In the case with the fixed transition density, the quark phase EOS connected to the hadronic phase with the NL3 is softer than that with the FSUGold, because of the larger bag constant. Meanwhile, due to the phase equilibrium in the mixed phase, the EOS initiated with the NL3 is softer than that with the FSUGold with increasing the density. Thus, the U-boson provides a more significant stiffening role in the EOS initiated with the stiff NL3 in the hadron phase.

Since in pure hadronic matter the stiffening effect of the U-boson is relevant to the extent of softness of the EOS's, it is interesting to examine whether such a dependence exists in the EOS of hybrid star matter with quark degrees of freedom. Shown in Fig. 3 is the EOS's of hybrid star matter with and without the contribution of the U-boson for two RMF parameter sets. We can see that after the occurrence of the hadron-quark phase transition, the difference in EOS's with the

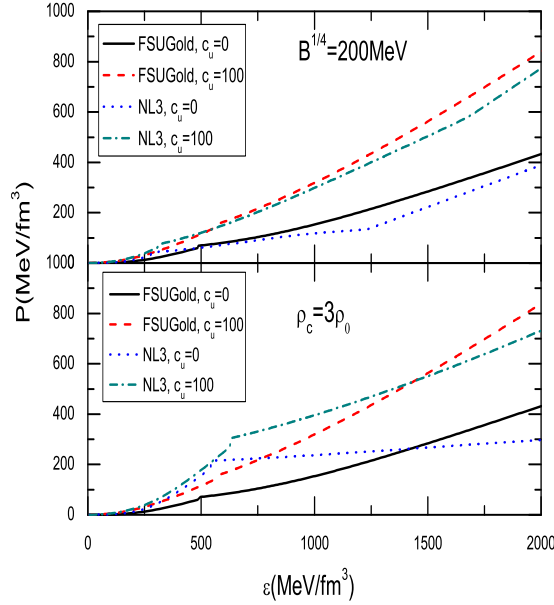


FIG. 3: (Color online) The influence of the U-boson on the EOS of hybrid star matter for different hadron phase models at the given bag constant  $B = (200 \text{ MeV})^4$  and transition density  $\rho_c = 3\rho_0$ , respectively.

fixed transition density seems to be more apparent than that with the fixed bag constant. This is understandable, because the different bag constants are used to obtain the same transition density. However, compared to the large difference in the EOS's in pure hadronic matter, as shown in Fig. 1, we see that the phase transition reduces the difference largely in EOS's at high densities. Compared to the evolution of EOS's with the NL3 and FSUGold, we see that the stiffer EOS undergoes a more appreciable softening of the EOS in the mixed phase, as the quark phase is given by the same MIT bag model either with the fixed bag constant or with a given transition density. We have also examined results for the bag constants ranging from 180 MeV to 220 MeV and transition densities from  $3\rho_0$  to  $4\rho_0$ . The increase of the bag constant or transition density gives rise to a larger extent of the mixed phase, consistent with that found in Ref. [89]. For instance, the transition density with  $B^{1/4} = 200 \text{ MeV}$  is  $0.28 \text{ fm}^{-3}$  with the parameter set NL3, the extent of the mixed phase increases from  $0.57 \text{ fm}^{-3}$  (with  $B^{1/4} = 180 \text{ MeV}$ ) to  $1.1 \text{ fm}^{-3}$ . With the parameter set FSUGold, the extent of the mixed phase gets a more apparent rise, and it is  $2.8 \text{ fm}^{-3}$  starting from the transition density  $0.47 \text{ fm}^{-3}$ . In any case, the appreciable stiffening role of the U-boson in the soft EOS's can be clearly observed as in Fig. 3, similar to that in Fig. 2.

In this work, we make comparative study with the stiff and soft EOS's. It is worthy to note the parameter  $\Lambda_v$  may also affect the EOS of asymmetric matter. The parameter  $\Lambda_v$  does not appear in the parameter set NL3. In the parameter set FSUGold, we may change this parameter (also change  $g_\rho$ ) by keeping the symmetry energy at saturation density unchanged. Here, we choose three parameter sets: FSUGw15 ( $\Lambda_v = 0.015$ ), FSUGlod ( $\Lambda_v = 0.03$ ), FSUGw45 ( $\Lambda_v = 0.045$ ), all of

which can fit the ground-state properties of  $^{208}\text{Pb}$  [3]. The transition density increases moderately with the rise of the  $\Lambda_v$ , since the stiffness of the symmetry energy that is controlled by the  $\Lambda_v$  can affect the chemical equilibrium. With the bag constant  $B^{1/4} = 180\text{MeV}$ , we obtain following transition densities:  $0.252$ ,  $0.282$ , and  $0.297\text{fm}^{-3}$  with the parameter sets FSUGw15, FSUGl0d and FSUGw45, respectively.

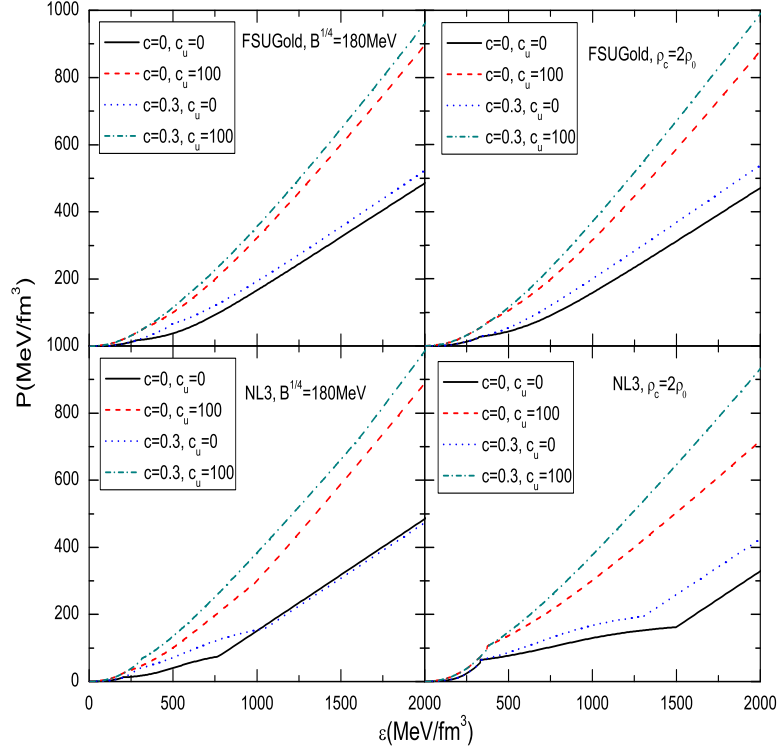


FIG. 4: (Color online) The EOS of hybrid star matter with the inclusion of the QCD correction ( $c = 0.3$ ) with and without the U-boson.

In above, the quarks with the bag model are free of interactions. As the QCD coupling is not negligible at densities of interest for compact star physics, it is here necessary to discuss briefly the QCD correction. It is reasonable to take the value of  $c$  in Eqs.(14),(15) to be 0.3 [26]. Shown in Fig. 4 is the EOS with the QCD correction. We see from Fig. 4 that the QCD correction can stiffen moderately the EOS of hybrid star matter at high densities. The QCD correction may affect the phase transition and increase the extent of the mixed phase due to the fact that the quark phase pressure is now modified by the QCD correction. For instance, with the bag constant  $B^{1/4} = 180\text{MeV}$ , the onset density of the mixed phase with the parameter set NL3 is then about  $0.28\text{fm}^{-3}$  with the extent of the mixed phase being about  $0.96\text{fm}^{-3}$ . With the parameter set FSUGold, the onset density of the mixed phase is about  $0.46\text{fm}^{-3}$ , and the extent of the mixed phase grows dramatically up to  $6.49\text{fm}^{-3}$ . As observed in Fig. 4, the QCD correction to the EOS is moderately dependent on

the hadron phase models. Specifically, the QCD correction results in an extent of the mixed phase with the soft FSUGold being larger than that with the stiff NL3. We should say that the specific dependence of the QCD correction on the hadron phase models is due to the connection built upon the phase equilibrium conditions. For comparisons, we also plot the results with and without the U-boson. As shown in Fig. 4, we see that the QCD correction is just moderate, compared with the contribution of the U-boson. The stiffening role of the U-boson is similar in cases with and without the QCD correction.

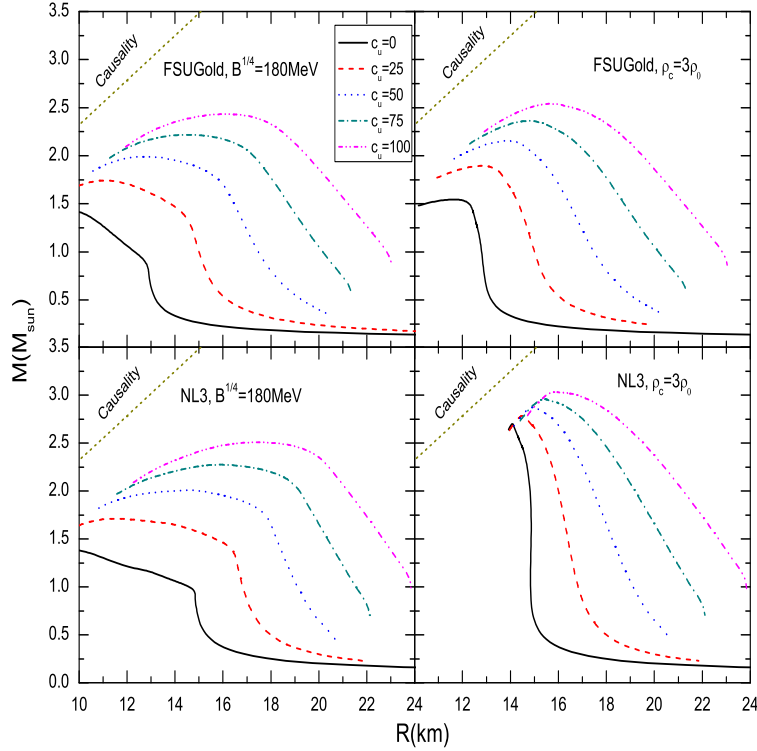


FIG. 5: (Color online) Mass-radius trajectories of hybrid stars with two hadron phase models. The U boson is included with various ratio parameters.

Now, we turn to the investigations of the hybrid star properties with these EOS's discussed above. Shown in Fig. 5 is the relationship between the NS mass and radius for various EOS's with the inclusion of the U-boson. For the stiff hadron phase EOS, the hadron-quark transition at a high density does not reduce the maximum mass of hybrid stars significantly, as shown in the lower right panel in Fig. 5. While in most cases, the phase transition may results in very significant reduction of the maximum mass, which should not be consistent with the observation of large mass NS's [18, 19]. We see that the inclusion of the U boson can remedy the mass eclipse very efficiently with the appropriately chosen ratio parameter. The rise of the maximum mass is consistent with the corresponding stiffening of the high-density EOS, shown in Fig. 2. We can see that the role of the

U-boson in increasing the maximum mass is more significant for softer EOS's.

Though shown in Fig. 5 are only the results with the particular bag constant and transition density, it is sufficient to reveal the role of the U-boson since the change of these parameters yields rather similar results. It is, however, interesting to examine the consequences in the internal structure of the particular NS by varying these parameters. Let's first make comparison to the results with  $B^{1/4} = 180$  and  $200$  MeV. With  $B^{1/4} = 180$  MeV, the parameter set NL3 gives a NS maximum mass  $1.39M_{\odot}$ . The size of the quark core is  $5.76$  km, the mixed phase spreads from  $5.76$  to  $7.62$  km, and the hadronic phase starts from  $7.62$  to  $9.68$  km. With  $B^{1/4} = 200$  MeV, the maximum mass is  $1.86M_{\odot}$ . For convenient comparison, we also examine the internal structure of the  $1.39M_{\odot}$  NS with  $B^{1/4} = 200$  MeV. The size of the quark core is now  $4.42$  km, the mixed phase spreads from  $4.42$  to  $6.38$  km, and the hadronic phase starts from  $6.38$  to  $10.59$  km. This indicates that the smaller bag constant that gives rise to a smaller transition density features a larger quark core in a particular NS. For the case with the smaller transition density, the conclusion is similar since the smaller transition density is given by the smaller bag constant.

It is also interesting to examine the effect of the U-boson on the NS structure, although the inclusion of the U-boson does not change the chemical and mechanical equilibriums, the transition densities, and the extents of each phases as well. As an example, here we examine the size of the quark core and of the mixed phase for the maximum mass configuration with the parameters  $B^{1/4} = 180$  MeV and  $(g_u/m_u)^2 = 25$  GeV<sup>-2</sup>. With the inclusion of the U-boson, the NS maximum mass increases from  $1.39M_{\odot}$  to  $1.71M_{\odot}$ . It is found in the NS with the maximum mass configuration that the radius of pure quark core is  $5.3$  km, which is smaller than  $5.76$  km obtained without the inclusion of the U-boson. The shell of the mixed phase extends from  $5.3$  to  $8.6$  km, while without the inclusion of the U-boson, the shell starts from  $5.76$  to  $7.6$  km. These results indicate that the U-boson may change the ratio of various phases in the particular NS though it does not take part in the phase transition.

As shown in Fig. 5, the NS radius is significantly increased by the U-boson. It was pointed out in the literature [6, 7] that the NS radius is primarily determined by the EOS in the lower density region of  $1\rho_0$  to  $2\rho_0$ . Since the inclusion of the U-boson also increases the pressure in the lower density region appreciably, a large extent of the NS radius is obtained accordingly with various  $c_u$ 's of interest. This is similar to the previous works in Ref. [37, 38]. It is known that the extraction of NS radii from observations still suffers from large systematic uncertainties [90] involved in the distance measurements and theoretical analyses of the light spectrum [8, 91–93]. There is yet no consensus on the extracted NS radii to date. For instance, using the thermal spectra from quiescent low-mass X-ray binaries (qLMXBs) Guillot and collaborators extracted NS radii of  $R_{\text{NS}} = 9.4 \pm 1.2$  km [94],

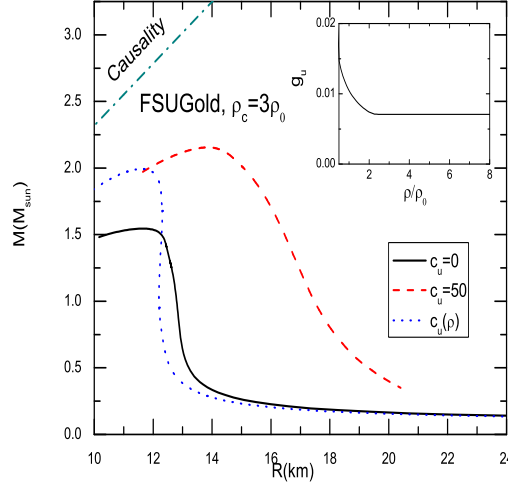


FIG. 6: (Color online) Mass-radius trajectories of hybrid stars with the hybrid EOS initiated with the FSUGold. The transition density is set to be  $3\rho_0$ . The dotted curve is the result with the density-dependent coupling constant of the U-boson, depicted in the inset. To obtain the density-dependent coupling, the mass of the U-boson is taken as  $1\text{MeV}$ .

while a relevant study of spectroscopic radius measurements also suggest small radii  $10.8^{+0.5}_{-0.4}$  km for a  $1.5 M_\odot$  NS [95]. There are also larger extracted radii: a  $3\text{-}\sigma$  lower limit of 11.1 km on the radius of the PSR J0437-4715 [96] and a lower limit of 13 km for 4U 1608-52 [97]. If the small radii of NS's is established, we need to reconsider the large NS radii produced by the U-boson. A possible solution of the NS radius suppression is to invoke the appropriate in-medium effects [98]. Considering that the NS radii are mainly determined by the low-density EOS, it is possible to reduce the NS radii by constructing the density-dependent coupling constant for the U-boson in the low-density regime. In the high-density regime, we neglect the in-medium effect for the U-boson, as one knows that the in-medium effect at high densities is suppressed greatly by the Pauli blocking [98, 100, 101]. As an example, we perform the calculation with the EOS whose hadron phase part is obtained with the FSUGold and find that the appropriate density-dependent coupling constant of the U-boson can reduce the NS radii significantly, as shown in Fig. 6. The density-dependent coupling constant, depicted in the inset of Fig. 6, is designed to little change the pressure in the low-density regime [98]. While the energy density still acquires a significant increase from the U-boson, the resulting NS radius is even less than the one obtained with the pure hadron phase EOS. Since the NS maximum mass is determined mainly by the high-density EOS, the present form of the density dependence just gives rise to a moderate reduction of the NS maximum mass.

In Figs. 5 and 6, we have not included the contribution of the QCD correction. The influence of the QCD correction on the NS maximum mass is rather sensitive to the transition density. Given large transition densities, the QCD correction just plays limited role in enhancing the NS maximum

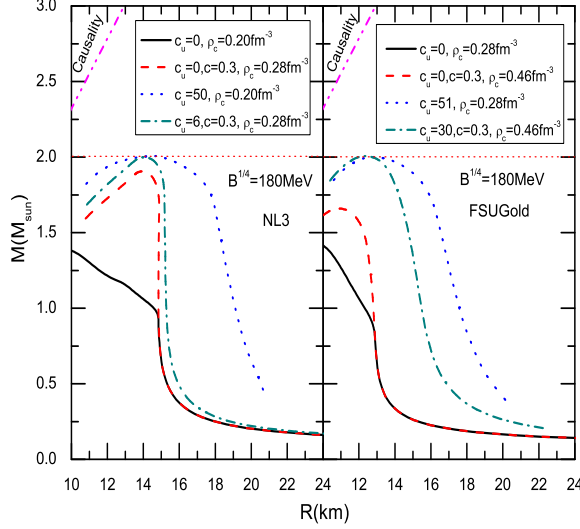


FIG. 7: (Color online) Mass-radius trajectories of hybrid stars with and without the QCD correction. To obtain the  $2M_{\odot}$  stars, the U-boson is also needed with the parameter denoted in the legend.

mass, since the maximum mass in this case is dominated by the hadron phase EOS. As the transition density decreases, the QCD correction brings more significant enhancement for the NS maximum mass. This findings are consistent with those in Ref. [32]. On the other hand, as we fix the bag constant, the situation for the QCD correction is different because the transition density itself in this case is increased by the correction through the phase equilibrium conditions. As shown in Fig. 7, the QCD correction with the fixed bag constant gives rise to a significant enhancement of the NS maximum mass, which is mainly attributed to the appreciable rise of the transition density. In this case, since the hadron phase EOS with the NL3 is much stiffer than that with the FSUGold, the large transition density due to the QCD correction leads to a more appreciable enhancement of the NS maximum mass with the NL3. With the inclusion of the U-boson, the NS maximum mass can further increase to satisfy the  $2M_{\odot}$  constraint [18, 19]. It is interesting to see that we just need a smaller ratio parameter of the U-boson to meet the maximum mass constraint in this case. This is more apparent for the EOS with the stiff NL3: the ratio parameter is largely reduced by the QCD correction, as shown in Fig. 7

Since the magnitude and in-medium behavior of the U-boson ratio parameter are important for the NS properties, it remains significant to discuss the parameters for the U-boson. To satisfy the NS maximum mass constraint, the ratio parameter  $c_u$  in this work is estimated to be around  $0 \sim 50 \text{ GeV}^{-2}$ , depending on the hadron phase models chosen. To avoid the violation of the low-energy nuclear constraints for finite nuclei, we may limit the weak interaction strength of the U-boson with the mass being of order  $1 \text{ MeV}$  [38, 98]. For instance, if  $g_u$  is 0.01, then the mass of the U-boson would be below  $1.4 \text{ MeV}$ , responsible for a long-range interaction. The weak interaction strength

of the U-boson does not compromise the success of nuclear models in reproducing the properties of finite nuclei [99]. Interestingly, the inclusion of the QCD correction may reduce the ratio parameter significantly. We note that these estimated orders of magnitude for the U-boson parameters can be compatible with parameter regions allowed by a few experimental constraints [36]. Moreover, the density-dependent parameter of the U-boson is found to be consistent with the usual predictions on the NS radius, while the density dependence would originate from the in-medium effect in the nuclear many-body system [98, 100, 101].

#### IV. SUMMARY

In this work, we have investigated the hadron-quark phase transition using the Gibbs conditions with the RMF models for hadron phase and MIT bag model for quark phase. We have considered the U-boson to stiffen the EOS of hybrid matter that is softened greatly by the phase transition. With the inclusion of the U-boson, the hybrid EOS is appreciably stiffened, and the stiffening extent is similar in the EOS's with stiff and soft hadron phase models due to the fact that the same MIT model is used for the quark phase. As a result, the NS maximum mass is significantly increased by the U-boson. In addition, we have investigated the effect of the effective QCD correction on the hybrid EOS. This correction may give rise to the stiffening of the hybrid EOS and the increase of the NS maximum mass that is significant as the transition density is not very high. The effective QCD correction can reduce the coupling strength of the U-boson that is needed to satisfy NS maximum mass constraint. While the inclusion of the U-boson also increases the NS radius significantly, we find that appropriate density dependence of the U-boson coupling constant may bring the NS radius down to the regime consistent with the observations and other model predictions. We have also discussed that with the weak interaction strength the inclusion of the U-boson does not compromise the success of conventional nuclear models in reproducing properties of finite nuclei. In summary, the inclusion of the U-boson can favorably allow the existence of quark degrees of freedom in the NS interior that is declined by the large mass NS observations. On the other hand, the future coincident measurements and more precise extraction of the mass and radius of neutron stars may also bring the constraint for the U-boson that is yet to be detected in the terrestrial laboratory.

#### Acknowledgement

The work was supported in part by the National Natural Science Foundation of China under Grant No. 11275048 and the China Jiangsu Provincial Natural Science Foundation under Grant No.



BK20131286.

- 
- [1] C. J. Horowitz and J. Piekarewicz, *Phys. Rev. Lett.* **86**, 5647 (2001).
  - [2] W. Z. Jiang, Z. Z. Ren, Z. Q. Sheng, and Z. Y. Zhu, *Eur. Phys. J. A* **44**, 465 (2010).
  - [3] W. Z. Jiang, *Phys. Rev. C* **81**, 044306 (2010).
  - [4] R. Wang and L. W. Chen, *Phys. Rev. C* **92**, 031303 (2015).
  - [5] B. A. Li and W. Udo Schroder (Eds.), *Isospin Physics in Heavy-Ion Collisions at Intermediate Energies*, Nova Science Publishers, New York, 2001.
  - [6] B. A. Li, L. W. Chen, and C. M. Ko, *Phys. Rep.* **464**, 113 (2008).
  - [7] J. M. Lattimer and M. Prakash, *Phys. Rep.* **333**, 121 (2000).
  - [8] J. M. Lattimer and M. Prakash, *Astrophys. J.* **550**, 426 (2001).
  - [9] J. M. Lattimer and M. Prakash, *Science* **304**, 536 (2004).
  - [10] J. M. Lattimer and M. Prakash, *Phys. Rep.* **442**, 109 (2007).
  - [11] A. W. Steiner, M. Prakash, J. M. Lattimer, and P. J. Ellis, *Phys. Rep.* **411**, 325 (2005).
  - [12] B. A. Li, W. J. Guo, and Z. Z. Shi, *Phys. Rev. C* **91**, 044601 (2015).
  - [13] P. Danielewicz, R. Lacey, and W. G. Lynch, *Science* **298**, 1592 (2002).
  - [14] B. A. Brown, *Phys. Rev. Lett.* **85**, 5296 (2000).
  - [15] L. W. Chen, C. M. Ko, and B. A. Li, *Phys. Rev. C* **72**, 064309 (2005).
  - [16] C. Fuchs and H. H. Wolter, *Eur. Phys. J. A* **30**, 5 (2006).
  - [17] L. W. Chen, C. M. Ko, and B. A. Li, *Phys. Rev. C* **76**, 054316 (2007).
  - [18] P. Demorest et al., *Nature* **467**, 1081 (2010).
  - [19] J. Antoniadis et al., *Science* **340**, 6131 (2013).
  - [20] J. E. Trumper, V. Burwitz, F. Haberl, and V. E. Zavlin, *Nucl. Phys. B Proc. Sup.* **132**, 560 (2004).
  - [21] F. Özel, *Nature* **441**, 1115 (2006).
  - [22] I. Bednarek, P. Haensel, J. Zdunik, M. Bejger, and R. Manka, *arXiv:1111.6942* (2011).
  - [23] W. Z. Jiang, B. A. Li, and L. W. Chen, *Astrophys. J.* **756**, 56 (2012).
  - [24] S. B. Ruster and D. H. Rischke, *Phys. Rev. D* **69**, 045011 (2004).
  - [25] J. E. Horvath and G. Lugones, *Astron. Astrophys.* **442**, L1 (2004).
  - [26] M. Alford, M. Braby, M. Paris, and S. Reddy, *Astrophys. J.* **629**, 969 (2005).
  - [27] M. Alford, D. Blaschke, A. Drago et al., *Nature*, **445**, 7 (2007).
  - [28] N. D. Ippolito, M. Ruggieri, D. H. Rischke, A. Sedrakian, and F. Weber, *Phys. Rev. D* **77**, 023004 (2008).
  - [29] T. Fischer, I. Sagert, G. Pagliara et al., *Astrophys. J. Suppl.* **194**, 39 (2010).
  - [30] A. Kurkela, P. Romatschke, and A. Vuorinen, *Phys. Rev. D* **81**, 105021 (2010).
  - [31] A. Kurkela, P. Romatschke, A. Vuorinen, and B. Wu, *arXiv:1006.4062* (2010).
  - [32] S. Weissenborn et al., *Astrophys. J.* **740**, L14 (2011).
  - [33] L. Bonanno and A. Sedrakian, *Astron. Astrophys.* **539**, A16 (2012).
  - [34] N. Yasutake, R. Lstowiecki, S. Benic, D. Blaschke et al., *Phys. Rev. C* **89**, 065803 (2014).
  - [35] C. J. Xia, G. X. Peng, S. W. Chen, Z. Y. Lu, and J. F. Xu, *Phys. Rev. D* **89**, 105027 (2014).
  - [36] M. I. Krivoruchenko, F. Simkovic, and A. Faessler, *Phys. Rev. D* **79**, 125023 (2009).
  - [37] D. H. Wen, B. A. Li, and L. W. Chen, *Phys. Rev. Lett.* **103**, 211102 (2009).
  - [38] D. R. Zhang, P. L. Yin, W. Wang, Q. C. Wang, and W. Z. Jiang, *Phys. Rev. C* **83**, 035801 (2011).
  - [39] P. Fayet, *Phys. Lett. B* **95**, 285 (1980).
  - [40] P. Fayet, *Phys. Lett. B* **172**, 363 (1986); *Nucl. Phys. B* **347**, 743 (1990).
  - [41] E. Fischbach and C. L. Talmadge, *The Search for Non-Newtonian Gravity* (Springer-Verlag, Inc., New York, 1999), ISBN 0-387-98490-9.
  - [42] E. G. Adelberger et al., *Annu. Rev. Nucl. Part. Sci.* **53**, 77 (2003).
  - [43] C. Boehm, D. Hooper, J. Silk, M. Casse, and J. Paul, *Phys. Rev. Lett.* **92**, 101301 (2004).
  - [44] S. H. Zhu, *Phys. Rev. D* **75**, 115004 (2007).
  - [45] P. Fayet, *Phys. Rev. D* **75**, 115017 (2007).
  - [46] P. Jean et al., *Astron. Astrophys.* **407**, L55 (2003); J. Knodlseder et al., *Astron. Astrophys.* **411**, L457 (2003).
  - [47] H. Zheng and L. W. Chen, *Phys. Rev. D* **85**, 043013 (2012).
  - [48] Z. G. Xiao, B. A. Li, L. W. Chen, G. C. Yong, and M. Zhang, *Phys. Rev. Lett.* **102**, 062502 (2009).
  - [49] J. D. Walecka, *Ann. Phys.(NY)* **83**, 491 (1974).
  - [50] J. Boguta and A. R. Bodmer, *Nucl. Phys. A* **292**, 423 (1977).
  - [51] S. A. Chin, *Ann. Phys.* **108**, 301 (1977).
  - [52] B. D. Serot and J. D. Walecka, *Adv. Nucl. Phys.* **16**, 1 (1986).
  - [53] P. G. Reinhard, *Rep. Prog. Phys.* **52**, 439 (1989).
  - [54] P. Ring, *Prog. Part. Nucl. Phys.* **37**, 193 (1996).
  - [55] B. D. Serot and J. D. Walecka, *Int. J. Mod. Phys. E* **6**, 515 (1997).
  - [56] M. Bender, P. H. Heenen, and P. G. Reinhard, *Rev. Mod. Phys.* **75**, 121 (2003).
  - [57] J. Meng, H. Toki, S. G. Zhou, S. Q. Zhang, W. H. Long, and L. S. Geng, *Prog. Part. Nucl. Phys.* **57**,

- 470 (2006).
- [58] W. Z. Jiang, B. A. Li, and L. W. Chen, Phys. Rev. C **76**, 054314 (2007); Phys. Lett. B **653**, 184 (2007).
  - [59] A. Chodos, R. L. Jaffe, K. Johnson, C. B. Thorn, and V. F. Weisskopf, Phys. Rev. D **9**, 3471 (1974).
  - [60] U. Heinz, P. R. Subramanian, H. Stocker, and W. Greiner, J. Phys. G **12**, 1237 (1986).
  - [61] N. K. Glendenning, Phys. Rev. D **46**, 1274 (1992).
  - [62] N. K. Glendenning, Phys. Rep. **342**, 393 (2001).
  - [63] C. Alcock, E. Farhi, and A. Olinto, Astrophys. J. **310**, 261 (1986).
  - [64] P. Haensel, J. L. Zdunik, and R. Schaeffer, Astron. Astrophys. **160**, 121 (1986).
  - [65] E. S. Fraga, R. D. Pisarski, and J. Schaffner-Bielich, Phys. Rev. D **63**, 121702 (2001).
  - [66] J. F. Xu, G. X. Peng, F. Liu, D. F. Hou, and L. W. Chen, Phys. Rev. D **92**, 025025 (2015).
  - [67] E. S. Fraga et al., Astrophys. J. **781**, L25 (2014).
  - [68] J. Oppenheimer and G. Volkoff, Phys. Rev. **55**, 374 (1939).
  - [69] R. C. Tolman, Phys. Rev. **55**, 364 (1939).
  - [70] G. Baym, C. Pethick, and P. Sutherland, Astrophys. J. **170**, 299 (1971).
  - [71] K. Iida and K. Sato, Astrophys. J. **477**, 294 (1997).
  - [72] , W. Z. Jiang, Phys. Lett. B **642**, 28 (2006).
  - [73] F. Yang and H. Shen, Phys. Rev. C **77**, 025801 (2008).
  - [74] J. Xu, L. W. Chen, C. M. Ko et al., Phys. Rev. C **81**, 055803 (2010).
  - [75] T. Takatsuka, S. Nishizaki, Y. Yamamoto, and R. Tamagaki, Prog. Theor. Phys. Suppl., **146**, 279 (2002).
  - [76] H. Chen, M. Baldo, G. F. Burgio et al., Phys. Rev. D **84**, 105023 (2011).
  - [77] G. A. Lalazissis, J. König, and P. Ring, Phys. Rev. C **55**, 540 (1997).
  - [78] B. G. Todd-Rutel and J. Piekarewicz, Phys. Rev. Lett. **95**, 122501 (2005).
  - [79] T. A. DeGrand, R. L. Jaffe, K. Johnson, and J. Kiskis, Phys. Rev. D **12**, 2060 (1975).
  - [80] J. Bartelski, A. Szymacha, Z. Ryzak, L. Mankiewicz, and S. Tatur, Nucl. Phys. **A424**, 484 (1984).
  - [81] M. Chanowitz and S. Sharpe, Nucl. Phys. B **222**, 211 (1983).
  - [82] C. E. Carlson, T. H. Hansson, and C. Peterson, Phys. Rev. D **27**, 1556 (1983).
  - [83] C. M. Ko and L. H. Xia, Phys. Rev. Lett. **62**, 1595 (1989).
  - [84] Z. J. He, et.al., Phys. Lett. B **495**, 317 (2000).
  - [85] W. Z. Jiang, R. Y. Yang, D. R. Zhang et al., Phys. Rev. C **87**, 064314 (2013).
  - [86] B. K. Sharma, et.al., Phys. Rev. C **75**, 035808 (2007).
  - [87] G.Y. Shao, M. Di Toro, B. Liu et al., Phys. Rev. D **83**, 094033 (2011).
  - [88] R. Cavagnoli, C. Providência, D. P. Menezes et al., Phys. Rev. C **83**, 045201 (2011).
  - [89] M. Prakash, I. Bombaci, M. Prakash, P. J. Ellis, J. M. Lattimer, and R. Knorren, Phys. Rep. **280**, 1 (1997).
  - [90] M. C. Miller, arXiv/1312.0029.
  - [91] P. Haensel, Astron. Astrophys. **380**, 186 (2001).
  - [92] C. M. Zhang, H. X. Yin, Y. Kojima, H. K. Chang et al., Mon. Not. Roy. Astron. Soc. **374**, 232 (2007).
  - [93] V. Suleimanov, J. Poutanen, M. Revnivtsev, and K. Werner, Astrophys. J. **742**, 122 (2011).
  - [94] S. Guillot and R. E. Rutledge, Astrophys. J. **796**, 1 (2014).
  - [95] F. Özel, D. Psaltis, T. Güver, G. Baym, C. Heinke, and S. Guillot, arXiv:1505.05155.
  - [96] S. Bogdanov, Astrophys. J. **762**, 96 (2013).
  - [97] J. Poutanen, J. Nättälä, J. J. E. Kajava et al., Mon. Not. Roy. Astron. Soc. **442**, 3777 (2014).
  - [98] W. Z. Jiang, B. A. Li, and F. J. Fattoyev, Eur. Phys. J. A **51**, 119 (2015).
  - [99] J. Xu, B. A. Li, L. W. Chen, H. Zheng, J. Phys. G **40**, 035107 (2013).
  - [100] R. Brockmann and H. Toki, Phys. Rev. Lett. **68**, 3408 (1992).
  - [101] Z. Y. Ma, H. L. Shi, and B. Q. Chen, Phys. Rev. C **50**, 3170 (1994).